Title:

Mixed Affinity Binding in Humans with 18 kDa Translocator Protein (TSPO) Ligands

Authors:

David RJ Owen[1,2], Roger N Gunn[2,3], Eugenii A Rabiner[2,3], Idriss Bennacef[2], Masahiro Fujita[4], William C Kreisl[4], Robert B Innis[4], Victor W Pike[4], Richard Reynolds[5], Paul M Matthews[2,3], Christine A Parker[2].

[1]Division of Experimental Medicine, Imperial College, Hammersmith Hospital, London W12 0NN, UK

[2]GSK Clinical Imaging Centre, London, W12 0NN, UK

[3]Centre for Neuroscience, Imperial College, London W12 0NN, UK

[4]Molecular Imaging Branch, National Institute of Mental Health, Bethesda, MD 20892, USA

[5]Wolfson Neuroscience Laboratories, Imperial College, London, UK

Running Title:

Mixed affinity binding with TSPO ligands

Corresponding Author:

Dr David RJ Owen

Experimental Medicine,

Imperial College, Hammersmith Hospital, London W12 0NN

Email: d.owen@imperial.ac.uk,

Tel: 0208 008 6116

This work is supported by GlaxoSmithKline, Imperial College and The Wellcome Trust. Robert B Innis, Masahiro Fujita and Victor W Pike acknowledge support from the Intramural Research Program of the National Institutes of Health (NIMH).

Abstract

[^{11}C]PBR28-PET can detect the 18kDa Translocator Protein (TSPO) expressed within macrophages. However, quantitative evaluation of the signal in brain tissue from donors with multiple sclerosis (MS) shows that PBR28 binds the TSPO with high (K_i~4nM), low (K_i~200nM) or mixed affinity (two sites with K_i~4nM and ~300nM). Our study tested whether similar binding behaviour could be detected 1) in brain tissue from donors with no history of neurological disease, 2) with TSPO-binding PET ligands other than [^{11}C]PBR28, 3) for TSPO present in peripheral blood and 4) with human brain PET data acquired *in vivo* with [^{11}C]PBR28. **Methods** The affinity of TSPO ligands was measured in human brain *post mortem* from donors with a history of MS (n=13), donors without any history of neurological disease (n=20) and in platelets from healthy volunteers (n=13). Binding potential estimates from 35 [^{11}C]PBR28 PET scans from an independent sample of healthy volunteers were analysed using a Gaussian mixture model. **Results** Three binding affinity patterns were found in brains from subjects without neurological disease in similar proportions to those reported previously from studies of MS brains. TSPO ligands showed substantial differences in affinity between subjects classified as high (HAB) and low affinity binders (LAB): differences in affinity between HABs and LABs are ~50-fold with PBR28, ~17-fold with PBR06, and ~4-fold with DAA1106, DPA713 and PBR111. Where differences in affinity between HABs and LABs were low (~4 fold), distinct affinities were not resolvable in binding curves for mixed affinity binders (MABs), who appeared to express one class of sites with an affinity approximately equal to the mean of those for HABs and LABs. Mixed affinity binding was detected in platelets from an independent sample (HAB 69%, MAB 31%), although LABs were not detected. Analysis of [^{11}C]PBR28 PET data was not inconsistent with the existence of distinct sub-populations of HABs, MABs and LABs. **Conclusions** With the exception of [^{11}C]PK11195, all TSPO PET ligands in current clinical

application recognise high, low and mixed-affinity binders in brain tissue *in vitro.* Knowledge of subjects' binding patterns will be required to accurately quantify TSPO expression *in vivo* using PET.

Keywords:

TSPO, mixed affinity binding

Introduction

The 18kDa Translocator Protein (TSPO) is expressed within microglia and macrophages and has been used as a target for positron emission tomography (PET) ligands to study disease processes that involve microglial activation or the recruitment of macrophages, such as multiple sclerosis (MS) and Alzheimer's disease *(1), (2)*. The PET radioligand [^{11}C]PK11195 has been used most frequently for this purpose, but signal quantification is limited by poor specific signal-to-background ratio *(1)*.

[^{11}C]PBR28 is a new high affinity TSPO PET radioligand with a more favourable specific to non-specific binding ratio than [^{11}C]PK11195 *(3)*. However, PET studies using [^{11}C]PBR28 have shown that approximately 10% of healthy volunteers do not show a specific binding signal in either the brain or peripheral organs *(4)*. Lymphocytes isolated from these subjects also have a marked reduction in affinity for PBR28 compared to the rest of the population, suggesting a global reduction in affinity of PBR28 for the TSPO *(5)*. This hypothesis is supported by our work using brain tissue donated predominantly from donors with an *ante mortem* diagnosis of MS, which found that a proportion of tissue samples (from donors designated "low affinity binders", LABs, approximately 23% of donors) demonstrated a reduced affinity for PBR28 (K_i~200nM) in comparison to donors designated "high affinity binders" (HABs, K_i~4nM, 46%) *(6)*. We also identified a third group of donors, designated "mixed affinity binders" (MABs, 31%), who showed behaviour consistent with the presence of two PBR28 binding sites in approximately equal number, with affinities similar to those of LABs and HABs (~4nM and ~300nM) *(6)*. In contrast to PBR28, PK11195 binds with similar affinity in all subjects, which may explain why non-binding has not been reported with this radioligand. It has not been established whether mixed affinity binding is a

phenomenon specific to MS or whether it also occurs in non-diseased brain tissue. It is also unknown whether mixed affinity binding is unique to brain tissue.

The presence of differing affinities in the general population complicates the quantitative assessment of PET data, because differences in [^{11}C]PBR28 signal cannot be safely interpreted as differences in target density. LABs are easily identifiable from a [^{11}C]PBR28 PET scan because their specific signal is negligible *(7)*. LABs are therefore easily eliminated from a cohort. MABs, however, cannot be distinguished from HABs in a single PET scan, although it may be possible to classify a subject's status by testing TSPO in blood and assuming that the binding affinity measured in peripheral blood reflects that in the brain. Population corrections then could be applied to compare subjects even when their binding affinities are different.

The phenomenon of low affinity binding has not been reported with other TSPO PET ligands currently in clinical use, such as [^{18}F]PBR111, [^{18}F]PBR06 *(8)*, [^{11}C]DPA713 *(9)* and [^{11}C]DAA1106 *(2)*. This may be because these ligands do not distinguish between HABs and LABs. Alternatively, it may be that differences in affinity exist but, because a PET signal is dependent upon both receptor density and affinity, the differences have not been recognised *in vivo*.

Our study had four aims. First, we tested whether the phenomenon of mixed affinity binding is restricted to MS or whether it is also found in neuropathologically normal brain tissue. Second, we examined whether the three binding patterns defined with PBR28 also are found with other TSPO ligands in clinical use. Third, we investigated whether it may be feasible to identify MABs from a peripheral blood assay by analysis of platelet binding. Finally, using a

set of [^{11}C]PBR28 PET brain scans acquired previously, we tested whether there is any evidence for mixed affinity binding in humans *in vivo*.

Materials and Methods

Human Tissue

Brain tissue

Tissue was obtained from the UK Multiple Sclerosis (MS) Tissue Bank at Imperial College. Of the 33 donors, 13/33 had been diagnosed with MS, and 20/33 had no history of neurological disease. All tissue blocks obtained included only "normal appearing" tissue, without immunohistochemical evidence of demyelination or significant inflammatory infiltrate. The tissue was stored at -80^{o}C until use. Demographic, tissue handling and clinical information concerning the donor is found in Suppl. Table 1a. The binding profiles for donors B1-B15 inclusive (13/15 with MS and 2/15 with no history of neurological disease) had been established previously using PBR28 *(6)*. Tissue from these donors was used to measure binding affinity with PBR06, PBR111, DPA713 and DAA1106. Due to tissue shortage, not all assays used all 15 donors. Tissue from donors B14-B33 inclusive (20/20 with no history of neurological disease) was used to estimate the proportions of the binding profiles in non-diseased brains.

Platelets

In an independent sample, 13 healthy volunteers (P1-P13) were recruited and venesection performed. These procedures were approved by the local Research Ethics Committee (Reference number 09/H0711/4). Demographic details concerning the volunteers are found in Suppl. Table 1b.

Materials

[^{3}H]PK11195(1-(2-Chlorophenyl)-*N*-methyl-*N*-(1-methylpropyl)-3-isoquinolinecarboxamide specific activity = 80 Ci/mmol; radioactive concentration = 1.0 mCi/ml) was purchased from Perkin Elmer, UK and [^{3}H]PBR28 (*N*-{[2-(methyloxy)phenyl]methyl}-*N*-[4-(phenyloxy)-3-pyridinyl]acetamide; specific activity = 82Ci/mmol; Radioactive concentration = 1.0mCi/ml) was custom labelled by G.E. Healthcare, UK. Unlabelled PK11195 was obtained from Sigma, UK; PBR06 and PBR111 were gifts from MNI, New Haven CT, USA. DPA713 and DAA1106 were synthesised in house according to described procedures *(10)*, *(11)*. [^{11}C]PBR28 for intravenous injection into human subjects was produced under a United States exploratory IND by ^{11}C-methylation of its *O*-desmethyl precursor as previously described (8).

Membrane preparation (brain tissue)

Tissue blocks were homogenised in 10 times weight for volume (w/v) buffer (0.32mM sucrose, 5mM Tris base, 1mM $MgCl_2$, pH 7.4, 4^{o}C). Homogenates were centrifuged (32,000*g*, 20min, 4^{o}C) followed by removal of the supernatant. Pellets were re-suspended in at least 10 times w/v buffer (50mM Tris base, 1mM $MgCl_2$, pH 7.4, 4^{o}C) followed by two washes by centrifugation (32,000*g*, 20min, 4^{o}C). Membranes were suspended in buffer (50mM Tris base, 1mM $MgCl_2$, pH 7.4, 4^{o}C) at a protein concentration of approximately 4 mg protein/ml and aliquots were stored at -80^{o}C until use.

Membrane preparation (platelets)

Whole blood (20ml) was collected from each volunteer into EDTA containing tubes, and centrifuged (180*g*, 15min, 4^{o}C). The supernatant (platelet-rich plasma) was collected and centrifuged (1800*g*, 15min, 4^{o}C). The supernatant was discarded and the platelet-containing pellet was stored at −80°C until use. Platelet pellets were homogenised in 10 times w/v buffer

(0.32mM sucrose, 5mM Tris base, 1mM $MgCl_2$, pH 7.4, 4°C). Homogenates were centrifuged (48,000*g*, 15min, 4°C) followed by removal of the supernatant. Pellets were re-suspended in at least 10 times w/v buffer (50mM Tris base, 1mM $MgCl_2$, pH 7.4, 4°C) followed by two washes by centrifugation (48,000*g*, 15min, 4°C). Membranes were suspended in buffer (50mM Tris base, 1mM $MgCl_2$, pH 7.4, 4°C) at a protein concentration of approximately 4 mg protein/ml and aliquots were stored at -80°C until use.

Competition binding assays

Aliquots (approximately 250µg protein/ml) of membrane suspension were prepared using assay buffer (50mM Tris base, 140mM NaCl, 1.5mM $MgCl_2$, 5mM KCl, 1.5mM $CaCl_2$, pH 7.4, 37°C) and incubated with [^{3}H]PK11195 (5nM) and one of 12 concentration of ligand (either PBR06, PBR111, DAA1106 or DPA713), ranging from 0.1nM to 300µM, in a final volume of 500µl for 60 min at 37°C. The specific binding component was determined using unlabelled PK11195 (10µM). Following incubation, assays were terminated via filtration through Whatman GF/B filters, followed by 3 x 1 ml washes with ice-cold wash buffer (50mM Tris Base, 1.4mM $MgCl_2$, pH 7.4, 4°C). Whatman GF/B filters were pre-incubated with 0.05% polyethyleneimine (60min) before filtration. Scintillation fluid (4ml/vial, Perkin Elmer Ultima Gold MV) was added and vials counted on a Perkin Elmer Tricarb 2900 liquid scintillation counter. For each donor, each point was performed in triplicate. K_i (nM) values were determined using GraphPad Prism 5.0 software (GraphPad Software Inc, USA). To measure the affinity of PBR111 for the low affinity site only, the assay was performed as above but with the addition of unlabeled PBR28 (50nM) in each well. At this concentration, PBR28 will occupy ~94% of binding sites in HABs and ~21% of binding sites in LABs. PBR111 was chosen for this assay as an example of a ligand which does not identify two binding sites in the MABs.

Protein concentration determination

Protein concentrations (μg protein/ml) were determined using the Bicinchoninic acid assay (BCA Kit, Sigma-Aldrich, UK) and absorption read at 562 nm.

Data analysis

All competition data were analysed using the iterative non-linear regression curve fitting software supplied with GraphPad Prism 5.0. Single site and two site competition models were fitted to the data using the least squares algorithm and model selection was performed using an F-test. The null hypothesis, that the data fitted a single site model, was rejected if the *p* value was less than 0.05. A K_d for [^{3}H]PK11195 of 29.25nM *(6)* was used to generate the K_i for PK11195, PBR28, PBR06, PBR111, DAA1106 and DPA713 according to the Cheng and Prusoff equation *(12)*. Subjects were classified by their behaviour in competition assays with PBR28: HABs were defined as subjects with a single class of binding sites with K_i <15nM, LABs were defined as subjects with a single class of binding sites with K_i >100nM, and MABs were defined as subjects with two binding sites. There were no subjects who showed a best fit to a single class of binding sites with between 15 and 100 nM. Data are expressed as the mean ± standard error of the mean (SEM). The Student's t-test (GraphPad Prism 5.0) was used to determine statistical significance.

Analysis of [^{11}C]PBR28 PET scans

35 healthy volunteers subjects (24/35 were male, age range 19-70 years, mean 41.4 years) who had undergone PET imaging with [^{11}C]PBR28 using Advance camera (GE Healthcare, USA), were analysed to determine whether there was evidence of multimodal distribution in the population. Parametric images of total volume of distributions (V_T) were created by the

Logan plot *(13)* using brain data acquired for 120min and metabolite-corrected arterial input function. After spatial normalization of the parametric images to the Montreal Neurological Institute space using coregistered T1-weighted MRI, V_T in the entire frontal cortex was obtained using the template developed by Tzourio-Mazoyer et al *(14)*. In addition, an associated measure of the plasma free fraction (f_P), derived from ultrafiltration *(4)*, allowed for the calculation of the volume of distribution in relation to the free plasma concentration (V_T/f_P). V_Ts from ~10% (3/35) of patients could not be determined because the specific signal was too low *(4)*; these patients are likely to represent LABs and this data was excluded from the following analysis. For the remaining subjects, a Gaussian mixture model was fitted separately to population estimates of V_T, f_P and V_T/f_P to investigate the likely number of components evident in the *in vivo* data. The method involved fitting a combination of univariate normal density functions to the data series, implemented in Matlab (Mathworks, Natick, USA). The data were fit with 1,2,3,4&5 Gaussians and the Akaike Information Criteria (AIC) was obtained to assist with model order determination (a lower AIC value indicating a more parsimonious model). Data is expressed as mean ± standard deviation.

Results

Detection of MABs in brain tissue donors with no history of neurological disease (donors B14-B33)

Binding affinity with PBR28 was measured in brain samples from 20 patients with no history of neurological disease (Fig.1). 9/20 (45%) bound to a single class of high affinity receptors (K_i=2.9±0.26nM) and were therefore classified as HABs. 4/20 (20%) bound to a single class of low affinity receptors (K_i =237 ± 35.0nM) and were classified as LABs. In 7/20 (35%), the data fitted best to a two site model with affinities of 3.6±2.0 nM and 1409±803nM. These subjects were classified as MABs. For the MABs, the mean fraction of high affinity sites was 58% ± 6.6%, with values ranging from 38-83%.

Estimation of PBR06 K_i in brain tissue (donors B1-B15)

Competition assays with unlabelled PBR06 were performed with tissue from 13 donors (Fig. 2). The mean K_i value for the HABs (8.6±2.0nM, n=5) was significantly lower than that of the LABs (149±46.6nM, n=4; $p<0.01$; Table 1). The K_i value for the high affinity MAB site (13.4±3.4nM, n=4) was similar to that of HABs, and the K_i value for the low affinity MAB site (176±103nM, n=4) was similar to that of LABs.

Estimation of DPA713 K_i in brain tissue (donors B1-B15)

Competition assays with unlabelled DPA713 were performed with tissue from 13 donors (Fig. 2). The mean K_i value for the HABs (15.0±2.2nM, n=5) was significantly lower than that of the LABs (66.4±7.8nM, n=4; $p<0.001$; Table 1). The data from all MABs were best described by a single site model, with a mean K_i value (26.8±2.9nM, n=4), which was similar to the mean K_i value of HABs and LABs (40.7nM).

Estimation of DAA1106 K_i in brain tissue (donors B1-B15)

Competition assay with unlabelled DAA1106 were performed with tissue from 12 donors (Fig. 2). The mean K_i value for the HABs (2.8±0.3nM, n=4) was significantly lower than that of the LABs (13.1±1.3nM, n=4; $p<0.001$; Table 1). For the MABs, all data fitted best to a single site model (4.8 0.4nM; n=4), which was similar to the mean K_i value of HABs and LABs (8.0nM).

Estimation of PBR111 K_i in brain tissue (donors B1-B15)

Competition assays with unlabelled PBR111 were performed with tissue from 14 donors (Fig. 2). The mean K_i value for the HABs (15.6±3.7nM, n=5) was significantly lower than that of the LABs (61.8±10.7nM, n=5; $p<0.003$; Table 1). The data from all MABs was best described by a single site model, with a mean K_i value (30.3±4.1nM, n=4), which was similar to the mean K_i value of HABs and LABs (38.7nM)

In the presence of 50nM PBR28

Because data from MABs with PBR111 was best described by a single site model, with a mean K_i value similar to the mean K_i value of HABs and LABs, we hypothesised that two sites were present in MABs but too close in affinity to resolve. To test this hypothesis the assays were repeated in the presence of PBR28 (50nM) in order to block the high affinity sites in all samples. For the HABs, the specific signal decreased by 70% following blockade with PBR28, rendering the signal to noise ratio too low to determine the affinity to the HAB site (Table 2). For the LABs, the specific signal dropped by 21% due to the PBR28 occupying a fraction of the LAB sites, but the K_i value did not significantly change (61.8±10.7nM to 51.7±12.2nM (n=4); (p=0.55); Table 2, Fig. 3)). For the MABs, the specific signal dropped by 49% and the K_i value increased significantly from 30.25±4.1nM, which is

similar to the mean K_i value of HABs and LABs, to 54.4±5.3nM (n=4, p<0.01), which is similar to the mean K_i value of the LABs (Fig. 3). Data from all patients was best described by a single site model.

Detection of MABs in platelets (Volunteers P1-P13)

Samples from 13 healthy volunteers were analysed with PBR28. In 9/13 (69%) the ligand bound to a single class of high affinity sites (K_i =3.1 ±0.57nM) and were therefore classified as HABs. In 4/13 (31%), the data fitted best to a two site model with affinities 1.1±0.40nM and 1266±988nM. These subjects were therefore classified as MABs. For the MABs, the mean fraction of high affinity sites was 63% ± 9.8%. In this cohort, no LABs were detected.

Analysis of PET data from healthy volunteers with [^{11}C]PBR28

In 3/35 [^{11}C]PBR28 PET scans, the V_T could not be calculated because the specific signal was too low. These subjects are likely to represent LABs. For the remaining subjects, the Gaussian mixture model indicated that the V_T was best described by a single component (Fig. 4), although AIC values were similar for both one and two component fits: AIC value = -61.939 (single component) vs -60.7238 (two components). The mean of the single component was 3.01 ± 1.03 and the means for the two components were 2.02 ± 0.46 and 3.78 ± 0.59 respectively. V_T/f_P was also best described by a single component, although again the AIC values were similar for both one and two component fits: AIC value = 38.148 (single component) vs 41.1452 (two components). The mean of the single component was 74.5 ± 23.6 and the means for the two components were 58.8 ± 13.2 and 97.4 ± 14.7 respectively. Regarding f_P, the mixture model predicted this was best described by two components; AIC value = -201.18 (single component) vs -204.239 (two components). There was no evidence that age and sex were responsible for the bimodal distribution of the f_P data.

Discussion

We have recently shown, using brain tissue from donors with MS, that PBR28 binds to a single class of high affinity sites in one group of patients (HABs), to a single class of low affinity sites in another group of patients (LABs) and with two distinct affinities in a third group of patients (MABs) *(6)*. These findings represent a challenge for quantitative [^{11}C]PBR28 PET studies of TSPO binding because the existence of patients with varying affinity for PBR28 means that differences in PET signal across subjects cannot be interpreted directly as differences in receptor density.

Here, we show that these three binding groups exist with similar frequencies in brain tissue from donors with no history of neurological disease (HAB 45%, MAB 35%, LAB 20%) as reported previously for donors having a history of MS (HAB 48%, MAB 32%, LAB 20%) *(6)*. We also show that such differences in affinity between groups of patients are not restricted to PBR28. The TSPO ligands PBR06, PBR111, DPA713 and DAA1106, all show differing affinities consistent with the presence of HABs and LABs. While differences in affinity are more pronounced with the phenoxyphenyl acetamides PBR28 and PBR06 (approximately 50 and 20-fold respectively), the differences are smaller with the phenylimidazopyridine PBR111 and its close relative, the phenylpyrazolopyrimidine, DPA713 (both ~ 4-fold). Predictions of this affinity ratio from structural class alone (Fig. 5), however, are imperfect: DAA1106, another phenoxyphenyl acetamide like PBR28, binds with similar high affinity to PBR28 in HABs, but exhibits a much smaller difference (~5-fold) between HABs and LABs. Since LABs have sufficient affinity with [^{18}F]PBR06, [^{11}C]DPA713, [^{18}F]PBR111 and [^{11}C]DAA1106 to produce a measurable signal in PET studies, their existence has gone undetected with these radioligands hitherto. However, their

reduction in affinity with respect to HABs means that TSPO expression in these patients will have been underestimated substantially.

The differing behaviour of MABs with each ligand provides pharmacological evidence that these subjects may co-express the same binding sites responsible for HAB and LAB behaviour. Two binding sites with distinguishable affinities were detected in MABs with both PBR28 and PBR06. With these ligands, the difference in affinity between the LAB site and HAB site is pronounced (>17-fold), and for each ligand the two affinities of the MABs were similar to those found with HABs and LABs. However, with PBR111, DAA1106 and DPA713, MABs appear to possess only one class of binding sites. With these ligands the HAB and LAB sites are very close in affinity (<5-fold) and for each ligand the affinity of the MABs was similar to the mean affinities of HABs and LABs. These data suggest that, for these three ligands, there may also be two classes of binding sites within tissue from MABs, whose affinities are too similar to resolve with this technique.

To test this hypothesis, PBR111 assays were repeated in the presence of PBR28 (50nM), a concentration chosen to block the majority of putative HAB sites whilst leaving most LAB sites unoccupied. The rationale was that the presence of the LAB site within MABs would be unmasked following blockade of the HAB site. Consistent with our model, the K_i of the LABs was unaffected; the K_i of the HABs could not be measured due to lack of signal, and the K_i of the MABs increased to align with that of the LABs. Furthermore, the specific signal obtained with the MABs dropped by approximately 50%. These data suggest that although PBR111 appears to bind a single class of receptors in all subjects, there are two distinct TSPO binding sites in MABs which are too similar in affinity to resolve. We therefore conclude that MABs possess HAB and LAB sites in approximately equal proportions, and

hypothesise that a) ligands with large differences in affinity between HABs and LABs will appear to bind two binding sites in MABs and b) ligands with small differences in affinity between HABs and LABs will appear to bind one class of binding sites in MABs, whose affinity is similar in magnitude to the mean of the HAB and LAB affinities.

Although our data suggest that most MABs express their two binding sites in approximately equal proportions, we note that the fraction of high affinity PBR28 binding sites within MABs ranges from 38 to 83%. Given the difficulties in detecting sites showing low expression, we cannot exclude the possibility that a continuum exists in expression of the HAB and LAB site. For example, it might be the case that all subjects that we have defined as HABs may express the LAB binding site (and vice versa), but do so at a level which is below the threshold of detection.

Having demonstrated that all the tested TSPO ligands can distinguish between HABs, MABs, and LABs, and that these groups exist in similar frequency in brain tissue from populations of donors with MS and with no history of neurological disease, we went on to address whether the three binding groups can be detected in peripheral blood. This addresses an important question for the future use of TSPO radioligands. If a peripheral blood assay can identify binding status, it would be possible to apply corrections to PET data allowing quantitative estimates of TSPO density between subjects in different binding groups. Alternatively, this approach could allow investigators to exclude subjects to ensure all participants within a study are from the same binding group. Using platelets isolated from healthy volunteers we found that approximately 30% of the samples were classified as MABs, a proportion which is consistent with our data from neuropathologically normal brains. We did not detect any LABs in this cohort, but given high affinity and low affinity binding has been shown in

peripheral lymphocytes *(15)*, this is likely to be a confound of limited power with our small sample. It remains to be demonstrated whether volunteers who are MABs with respect to their peripheral blood cells are also MABs with respect to their brain tissue, although again this has been demonstrated for PBR28 with HABs and LABs *(16)*.

Finally, we investigated whether mixed affinity binding occurs *in vivo* by analysing the distribution of V_T and V_T/f_P data from 35 [^{11}C]PBR28 PET scans. Having excluded 3 subjects with negligible signal who were likely to be LABs, our hypothesis was that the remaining data would contain two populations, representing HABs and MABs. Assuming identical TSPO expression across all subjects and low non-specific signal, the means of these two populations would be expected to differ by a factor of approximately 2. Although the mixture model preferred a single component fit for both V_T and V_T/f_P, the AIC values for a single component and a two component fit were similar. Given that TSPO expression will not be identical across subjects and that this will also affect V_T and V_T/f_P, we conclude that there is evidence for HABs and MABs *in vivo*. Furthermore, when the data were fitted to two components the means of these components differed by a factor of 1.9 for V_T and 1.7 for V_T/f_P, consistent with the hypothesis that the components represent HABs and MABs. Further investigation will be required to definitely demonstrate the existence of mixed affinity binding in the brain *in vivo*. Of note, the f_P data was distributed bimodally. This was an unexpected finding because plasma is not thought to contain TSPO binding sites, and we found no evidence that it was driven by age or sex. The reason for this bimodal distribution of f_P is unclear.

The distribution volume for a radioligand is given by $V_T = V_{ND} (1 + BP_{ND})$. Thus, by considering the affinity ratio ($R= K_{d\text{-}LAB}/K_{d\text{-}HAB}$), it is possible to calculate the ratio of the

binding potential (BP_{ND}) between the three groups (HABs, MABs and LABs) and consequently consider the impact on V_T. Assuming a 50:50 split of the total Bmax in the MAB, then the binding potential are given by ;

$$BP_{ND}^{LAB} = \frac{f_{ND} B_{\max}}{K_d^{HAB}} \left(\frac{1}{R} \right)$$

$$BP_{ND}^{MAB} = \frac{f_{ND} B_{\max}}{K_d^{HAB}} \left(\frac{R+1}{2R} \right)$$

$$BP_{ND}^{HAB} = \frac{f_{ND} B_{\max}}{K_d^{HAB}}$$

where:

f_{ND} = free fraction of radioligand in the non displaceable compartment

B_{max} = receptor density

Where a ligand shows little selectively between HABs and LABs, as with [^{11}C]PK11195, R will approach 1 and the expected binding potential will be the same for the three groups. For a highly selective ligand, such as [^{11}C]PBR28, the influence of the LAB site diminishes and the binding potential approaches 0.5 x $B_{max}/K_{d\text{-}HAB}$. Table 3 displays the R value for each of the ligands and predicts the ratio of specific signal that would be expected in HABs, MABs, and LABs with equal TSPO expression. The absolute BP_{ND} obtained will also depend on the f_{ND} which will likely differ for each ligand.

Conclusion

We thus have shown that, apart from PK11195, all TSPO PET ligands in clinical use recognise high-affinity, low-affinity and mixed-affinity binders in brain tissue *in vitro*. Whilst the same binding classes are evident from peripheral blood, it remains to be conclusively demonstrated that binding status in peripheral blood predicts that of the brain. Knowledge of binding status will be required to correctly quantify TSPO expression with PET.

Acknowledgements

The authors thank the UK Multiple Sclerosis Tissue Bank and Chris Rhodes for providing all human tissue used in this study.

Reference List

(1) Banati RB, Newcombe J, Gunn RN et al. The peripheral benzodiazepine binding site in the brain in multiple sclerosis: quantitative in vivo imaging of microglia as a measure of disease activity. *Brain*. 2000;123 (Pt 11):2321-2337.

(2) Yasuno F, Ota M, Kosaka J et al. Increased binding of peripheral benzodiazepine receptor in Alzheimer's disease measured by positron emission tomography with [11C]DAA1106. *Biol Psychiatry*. 2008;64(10):835-841.

(3) Imaizumi M, Briard E, Zoghbi SS et al. Brain and whole-body imaging in nonhuman primates of [11C]PBR28, a promising PET radioligand for peripheral benzodiazepine receptors. *Neuroimage*. 2008;39(3):1289-1298.

(4) Fujita M, Imaizumi M, Zoghbi SS et al. Kinetic analysis in healthy humans of a novel positron emission tomography radioligand to image the peripheral benzodiazepine receptor, a potential biomarker for inflammation. *Neuroimage*. 2008;40(1):43-52.

(5) Kreisl WC, Fujita M, Fujimura Y et al. Comparison of [(11)C]-(R)-PK 11195 and [(11)C]PBR28, two radioligands for translocator protein (18 kDa) in human and monkey: Implications for positron emission tomographic imaging of this inflammation biomarker. *Neuroimage*. 2009.

(6) Owen DR, Howell OW, Tang SP et al. Two binding sites for [(3)H]PBR28 in human brain: implications for TSPO PET imaging of neuroinflammation. *J Cereb Blood Flow Metab*. 2010.

(7) Kreisl WC, Fujita M, Fujimura Y et al. Comparison of [(11)C]-(R)-PK 11195 and [(11)C]PBR28, two radioligands for translocator protein (18 kDa) in human and monkey: Implications for positron emission tomographic imaging of this inflammation biomarker. *Neuroimage*. 2009.

(8) Fujimura Y, Zoghbi SS, Simeon FG et al. Quantification of translocator protein (18 kDa) in the human brain with PET and a novel radioligand, (18)F-PBR06. *J Nucl Med*. 2009;50(7):1047-1053.

(9) Endres CJ, Pomper MG, James M et al. Initial evaluation of 11C-DPA-713, a novel TSPO PET ligand, in humans. *J Nucl Med*. 2009;50(8):1276-1282.

(10) Okubo T, Yoshikawa R, Chaki S, Okuyama S, Nakazato A. Design, synthesis and structure-affinity relationships of aryloxyanilide derivatives as novel peripheral benzodiazepine receptor ligands. *Bioorg Med Chem*. 2004;12(2):423-438.

(11) Selleri S, Gratteri P, Costagli C et al. Insight into 2-phenylpyrazolo[1,5-a]pyrimidin-3-yl acetamides as peripheral benzodiazepine receptor ligands: synthesis, biological evaluation and 3D-QSAR investigation. *Bioorg Med Chem*. 2005;13(16):4821-4834.

(12) Cheng Y, Prusoff WH. Relationship between the inhibition constant (K1) and the concentration of inhibitor which causes 50 per cent inhibition (I50) of an enzymatic reaction. *Biochem Pharmacol*. 1973;22(23):3099-3108.

(13) Logan J, Fowler JS, Volkow ND et al. Graphical analysis of reversible radioligand binding from time-activity measurements applied to [N-11C-methyl]-(-)-cocaine PET studies in human subjects. *J Cereb Blood Flow Metab*. 1990;10(5):740-747.

(14) Tzourio-Mazoyer N, Landeau B, Papathanassiou D et al. Automated anatomical labeling of activations in SPM using a macroscopic anatomical parcellation of the MNI MRI single-subject brain. *Neuroimage*. 2002;15(1):273-289.

(15) Kreisl WC, Fujita M, Fujimura Y et al. Comparison of [(11)C]-(R)-PK 11195 and [(11)C]PBR28, two radioligands for translocator protein (18 kDa) in human and monkey: Implications for positron emission tomographic imaging of this inflammation biomarker. *Neuroimage*. 2009.

(16) Kreisl WC, Fujita M, Fujimura Y et al. Comparison of [(11)C]-(R)-PK 11195 and [(11)C]PBR28, two radioligands for translocator protein (18 kDa) in human and monkey: Implications for positron emission tomographic imaging of this inflammation biomarker. *Neuroimage*. 2009.

Table 1
Competition Binding Studies: K_i for HABs LABs and MABs with PK11195, PBR28, PBR06, PBR111, DPA713 and DAA1106

	Ki (nM) of PK11195*	Ki (nM) of PBR28*	Ki (nM) of PBR06	Ki (nM) of DPA713	Ki (nM) of DAA1106	Ki (nM) of PBR111
HABs	**28.3 ± 4.0 (n=6)**	**3.4 ± 0.2 (n=6)**	**8.6 ± 2.0 (n=5)**	**15.0 ± 2.2 (n=5)**	**2.8 ± 0.3 (n=4)**	**15.6 ± 3.7 (n=5)**
LABs	**22.3 ± 2.2 (n=5)**	**188 ± 7.0 (n=5)**	**149 ± 46.6 (n=4)**	**66.4 ± 7.7 (n=4)**	**13.1 ± 1.3 (n=4)**	**61.8 ± 10.7 (n=5)**
MABs	**23.6 ± 5.5 (n=4)**	**Two receptors detected (n=4)** **4.0 ± 1.2** (High) **313 ± 38** (Low)	**Two receptors detected (n=4)** **13.4 ± 3.4** (High) **176 ± 103** (Low)	**26.8 ± 2.9 (n=4)**	**4.8 ± 0.4 (n=4)**	**30.3 ± 4.1 (n=4)**
Ki ratio LAB: HAB	***0.8***	***55***	***17***	***4.4***	***4.7***	***4.0***
T-test HAB vs LAB	***p*<0.25**	**p < 0.0001**	**p<0.011**	**p<0.001**	**p<0.001**	**p<0.003**
T-test MAB vs LAB	***p*<0.82**	**N/A**	**N/A**	**p<0.003**	**p<0.001**	**p<0.04**
T-test MAB vs HAB	***p*<0.50**	**N/A**	**N/A**	**p<0.01**	**p<0.005**	**p<0.03**

Abbreviations: LABs; Low affinity binders. HABs; High affinity binders. MABs; Mixed affinity binders.
Figures are expressed as mean ± standard error of mean. .
All data in Table 1 were generated from donors B1-B15 inclusive
*Data reproduced from Owen et al *(6)*

Table 2
Competition Binding Studies: K_i for HABs LABs and MABs with PBR111 in the absence and presence of 50nM PBR28

	Ki (nM) of PBR111	Ki (nM) of PBR111following block with PBR28 (50nM)	Reduction (%) in specific signal following block with PBR28 (50nM)
HABs	**15.6 ± 3.7 (n=5)**	Not measurable	**69.0 ± 4.6 (n=4)**
LABs	**61.8 ± 10.7 (n=5)**	**51.7 ± 12.2 (n=4)**	**21.2 ± 4.8 (n=4)**
MABs	**30.25 ± 4.1 (n=4)**	**54.4 ± 5.3 (n=4)**	**49.3 ± 2.9 (n=4)**
T-test HAB vs LAB	**p<0.003**	N/A	***p*<0.0004**
T-test MAB vs LAB	**p<0.04**	***p*<0.84**	***p*<0.002**
T-test MAB vs HAB	**p<0.03**	N/A	***p*<0.01**

Abbreviations: LABs; Low affinity binders. HABs; High affinity binders. MABs; Mixed affinity binders.
Figures are expressed as mean ± standard error of mean.

Table 3
Ratio of specific signal for HABs, MABs and LABs with different TSPO ligands.

Ligand	LAB	MAB	HAB
PBR28	1	28.2	55.3
PBR06	1	9.2	17.3
DAA1106	1	2.9	4.7
PBR111	1	2.5	4.0
DPA173	1	2.7	4.4
PK11195	1	0.9	0.8

MABs are assumed to express an equal number of HAB and MAB sites.
Receptor density is assumed to remain constant.
Values are calculated as BP_{ND} relative to BP_{ND} of LABs.

Figure Legends

Figure 1

Competition assay with [^{3}H]PK11195 and unlabelled PBR28, using tissue from donors with no history of neurological disease. Each data point represents the mean value of all subjects, and the error bars represent SEM.
Abbreviations:
HABs; High affinity binders.
LABs; Low affinity binders.
MABs; Mixed affinity binders.

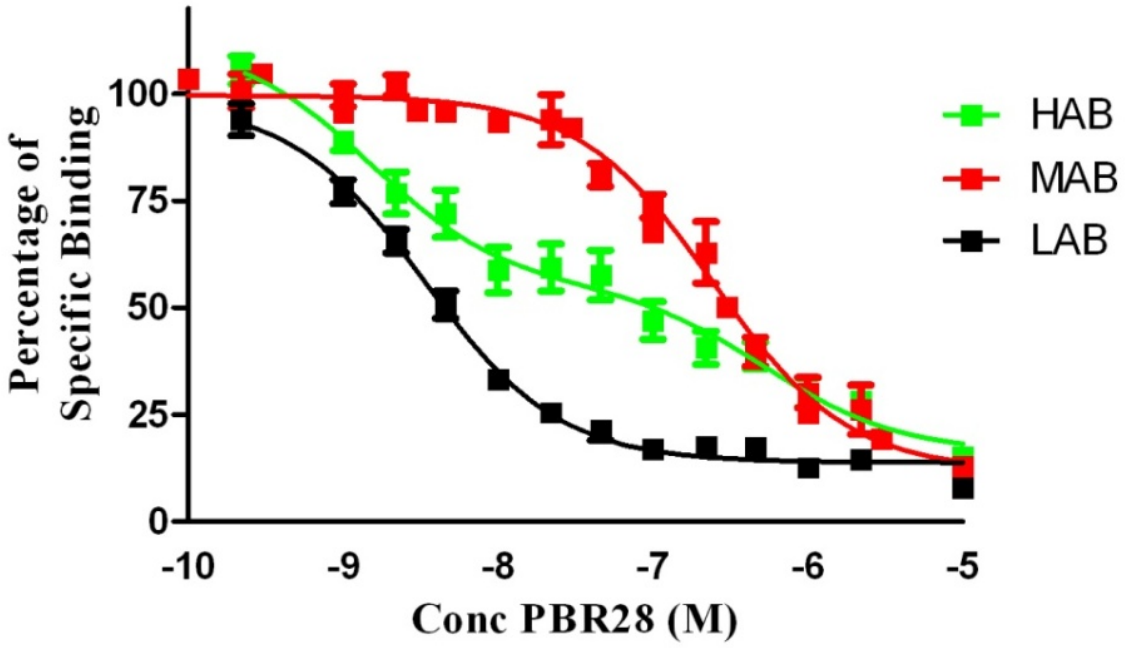

Figure 2

Competition assays with [^{3}H]PK11195 and unlabelled TSPO ligand using brain tissue previously characterised as HAB, LAB or MAB by PBR28 assays. Each data point represents the mean value of at least 4 subjects, and the error bars represent SEM.

Panel A **Phenoxyphenyl acetamid derivatives**
Panel B **Bi-cyclic linker derivatives**
Panel C **Phenyl –isoquinolinecarboxamide derivatives**

Abbreviations:
HABs; High affinity binders.
LABs; Low affinity binders.
MABs; Mixed affinity binders.
SB; specific binding.
SEM; standard error of mean

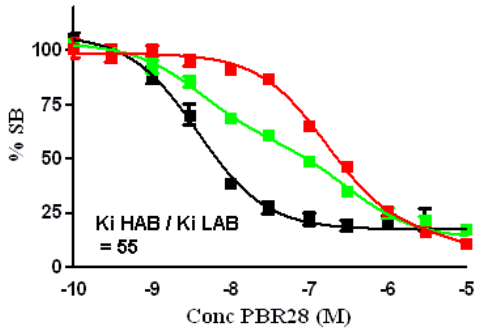
% SB
Ki HAB / Ki LAB
= 55
Conc PBR28 (M)

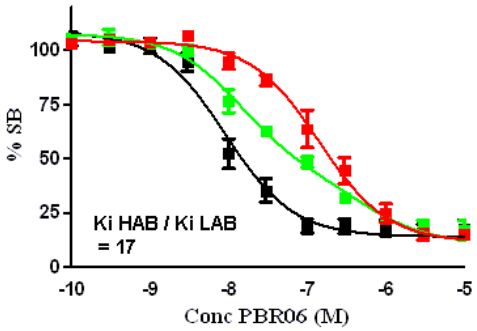
% SB
Ki HAB / Ki LAB
= 17
Conc PBR06 (M)

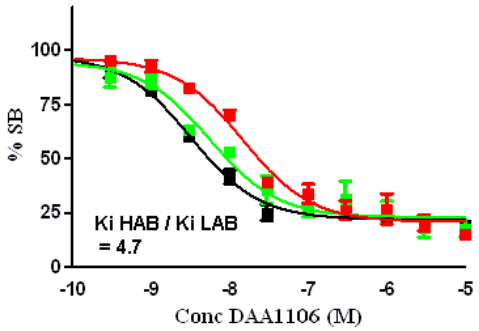
% SB
Ki HAB / Ki LAB
= 4.7
Conc DAA1106 (M)

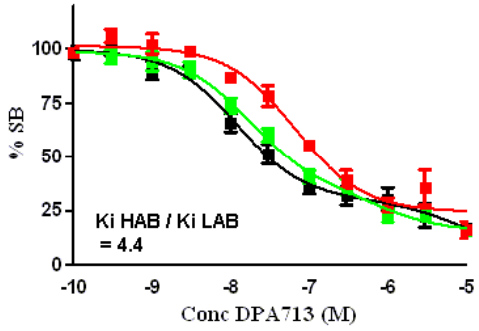
% SB
Ki HAB / Ki LAB
= 4.4
Conc DPA713 (M)

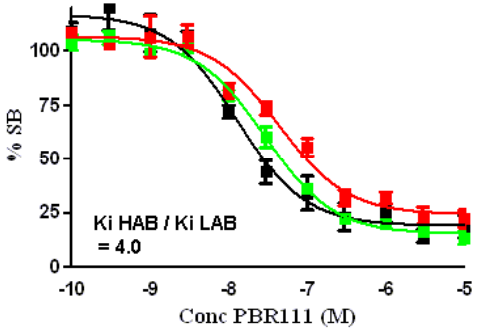
% SB
Ki HAB / Ki LAB
= 4.0
Conc PBR111 (M)

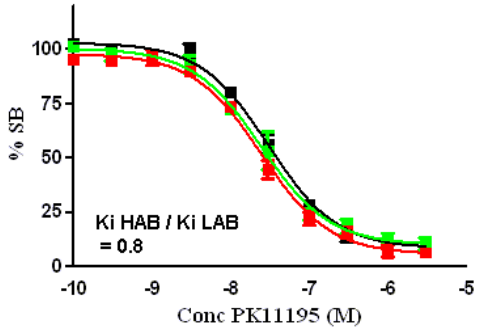
% SB
Ki HAB / Ki LAB
= 0.8
Conc PK11195 (M)

HAB
MAB
LAB

Figure 3

Competition assays with [^{3}H]PK11195 and unlabelled PBR111 in the presence or absence of PBR28 (50nM).

Abbreviations:
HABs; High affinity binders.
LABs; Low affinity binders.
MABs; Mixed affinity binders.

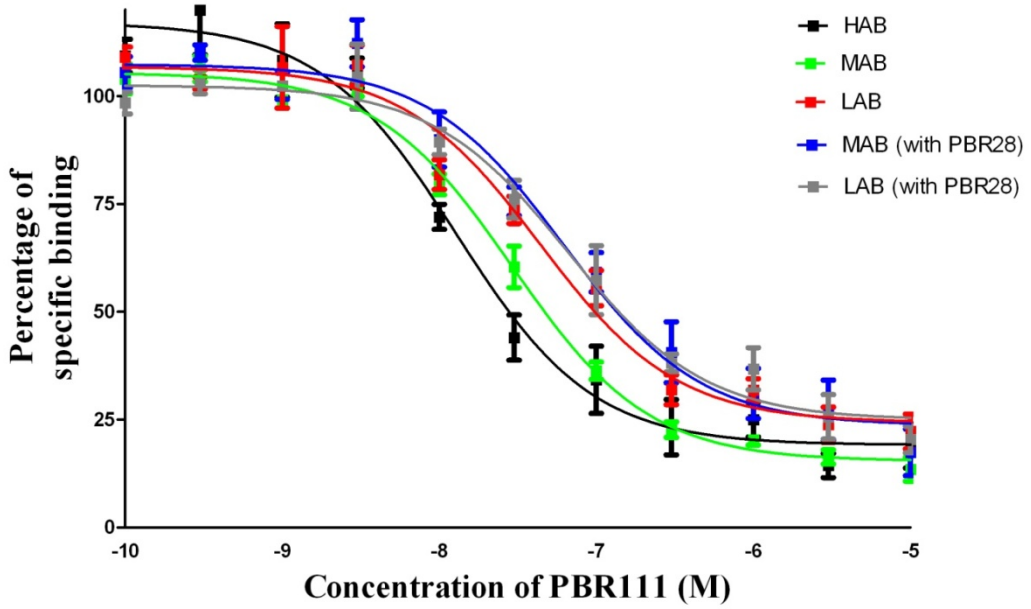

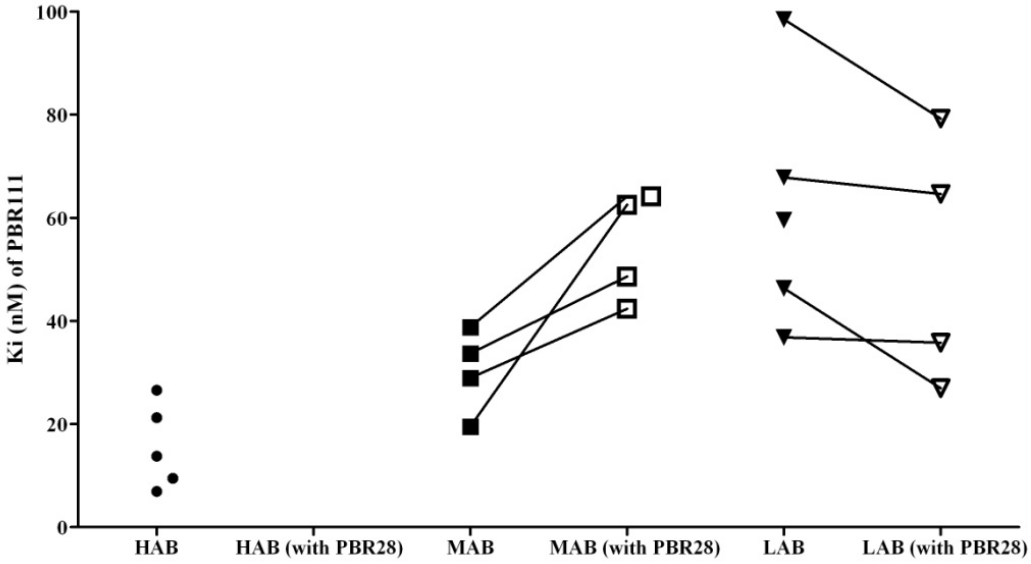

Figure 4

[^{11}C] PBR28 PET data from 32 healthy volunteers expressed as a histogram with a mixture model analysis showing two distributions for each measurement.

.

Panel A: Volume of distribution.
Panel B: Plasma free fraction.
Panel C: Volume of distribution / Plasma free fraction.

The blue curves denote the single component solutions, and the green and black curves denote the two component solutions. For the two component solutions, while different individuals are within each Gaussian group (e.g., green) for the three parameters, there was good agreement between panels A and B (74%) and A and C (66%).

A

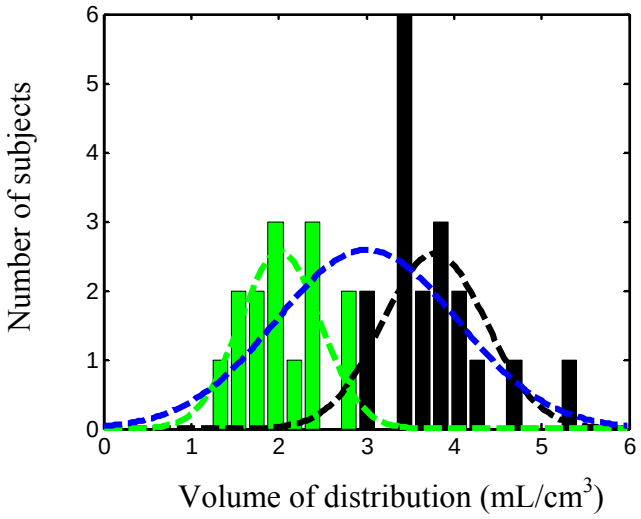

B

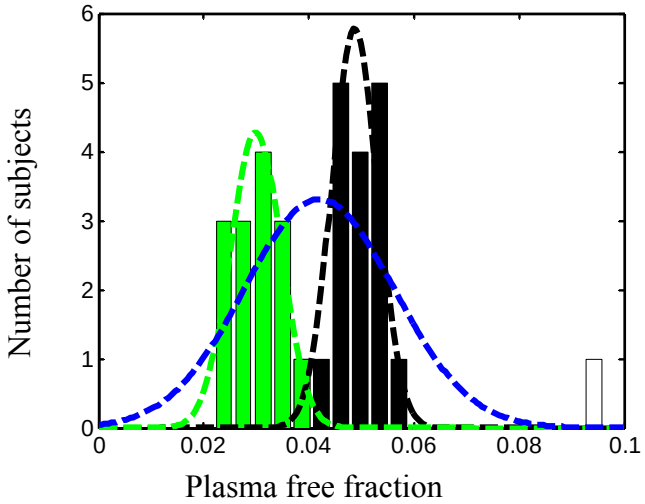

C

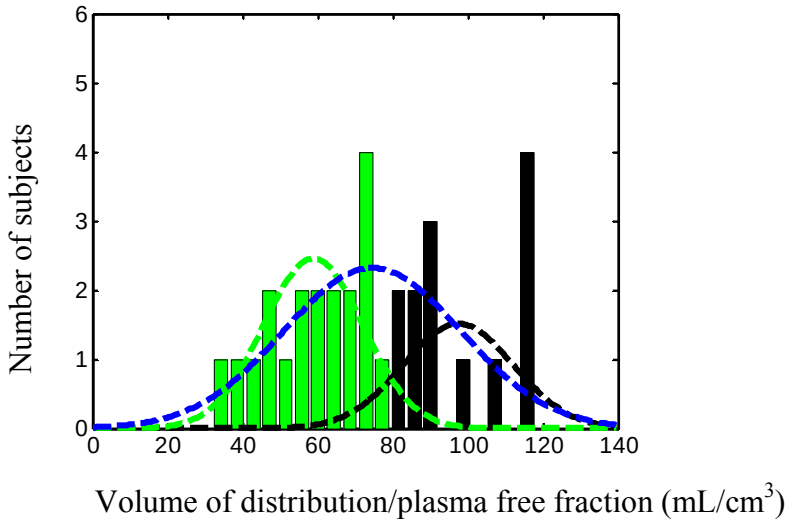
Number of subjects
0
1
2
3
4
5
6
0
20
40
60
80
100
120
140
Volume of distribution/plasma free fraction (mL/cm3)

Figure 5
TSPO ligands displayed in structural classes.

Phenoxyphenyl acetamid derivatives

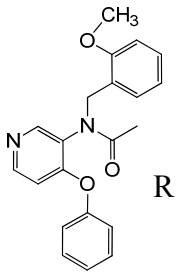

R = 55

PBR28

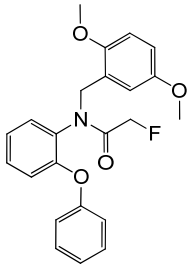

R = 17

PBR06

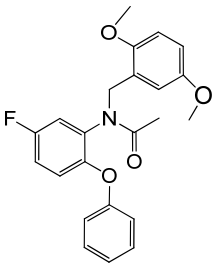

R = 4.7

DAA1106

Bicyclic linker derivatives

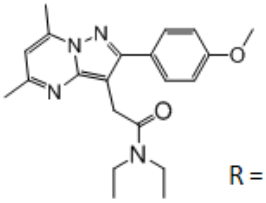

R = 4.4

DPA713

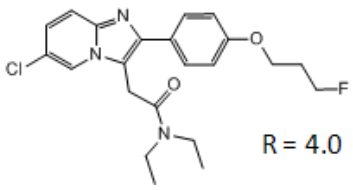

R = 4.0

PBR111

Phenyl–isoquinolinecarboxamide derivative

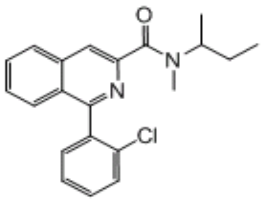

R = 0.8

PK11195